

AD-A051 127

AIR FORCE GEOPHYSICS LAB HANSCOM AFB MASS
INTERACTION OF A TURBULENT PLANAR HEATED JET WITH A COUNTERFLOW--ETC(U)
SEP 77 M M KLEIN
AFGL-TR-77-0214

F/G 4/2

UNCLASSIFIED

NL

1 OF 1
ADA
051127



END
DATE
FILMED
4 -78
DDC

ADA051127

AFGL-TR-77-0214
AIR FORCE SURVEYS IN GEOPHYSICS, NO. 375



2
B.S.

Interaction of a Turbulent Planar Heated Jet With a Counterflowing Wind

MILTON M. KLEIN

AD NO. 1
DDC FILE COPY

26 September 1977

DDC
RECEIVED
MAR 13 1978
B

Approved for public release; distribution unlimited.

METEOROLOGY DIVISION PROJECT 2093
AIR FORCE GEOPHYSICS LABORATORY
HANSCOM AFB, MASSACHUSETTS 01731

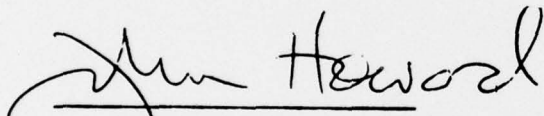
AIR FORCE SYSTEMS COMMAND, USAF



This report has been reviewed by the ESD Information Office (OI) and is releasable to the National Technical Information Service (NTIS).

This technical report has been reviewed and is approved for publication.

FOR THE COMMANDER



Chief Scientist

Qualified requestors may obtain additional copies from the Defense Documentation Center. All others should apply to the National Technical Information Service.

9 Air Force surveys in geophysics,

Unclassified

SECURITY CLASSIFICATION OF THIS PAGE (When Data Entered)

REPORT DOCUMENTATION PAGE		READ INSTRUCTIONS BEFORE COMPLETING FORM
1. REPORT NUMBER AFGL-TR-77-0214	2. GOVT ACCESSION NO. AFGL-AFSG-3751	3. RECIPIENT'S CATALOG NUMBER
4. TITLE (and Subtitle) INTERACTION OF A TURBULENT PLANAR HEATED JET WITH A COUNTERFLOWING WIND.	5. TYPE OF REPORT & PERIOD COVERED Scientific. Interim.	
7. AUTHOR(s) Milton M. Klein	6. PERFORMING ORG. REPORT NUMBER AFSG No. 375	
9. PERFORMING ORGANIZATION NAME AND ADDRESS Air Force Geophysics Laboratory (LYP) Hanscom AFB Massachusetts 01731	8. CONTRACT OR GRANT NUMBER(s)	
11. CONTROLLING OFFICE NAME AND ADDRESS Air Force Geophysics Laboratory (LYP) Hanscom AFB Massachusetts 01731	10. PROGRAM ELEMENT PROJECT TASK AREA & WORK UNIT NUMBERS 62101F 20930102	17. PI
14. MONITORING AGENCY NAME & ADDRESS (if different from Controlling Office)	11. REPORT DATE 26 Sep 1977	13. NUMBER OF PAGES 30
16. DISTRIBUTION STATEMENT (of this Report) Approved for public release; distribution unlimited.	15. SECURITY CLASS. (of this report) Unclassified	
17. DISTRIBUTION STATEMENT (of the abstract entered in Block 20, if different from Report)	15a. DECLASSIFICATION/DOWNGRADING SCHEDULE 12/29 p	
18. SUPPLEMENTARY NOTES	DDC RECEIVED MAR 13 1978 RECEIVED B	
19. KEY WORDS (Continue on reverse side if necessary and identify by block number) Thermal fog dispersion Counterflowing jet Heated jet Planar jet Turbulence		
20. ABSTRACT (Continue on reverse side if necessary and identify by block number) Experimental and theoretical programs are being conducted to aid in the development of an operational warm fog dispersal system using momentum-driven ground-based heat sources. In previous investigations, the wind was in the same direction as the jet (coflowing). The present investigation is concerned with a jet opposite in direction to the ambient wind (counterflowing or opposing jet). A model for calculating the dynamic characteristics of a cold counterflowing jet has been extended to take account of the effect of heating upon the		

1
409 578
Dal

Unclassified

SECURITY CLASSIFICATION OF THIS PAGE(When Data Entered)

20. Abstract (Continued)

jet. The effect of buoyancy upon the motion of the jet will be presented in a subsequent report.

The calculated velocity and temperature distributions are in fair to good agreement with the corresponding experimental results. In general, the calculated results drop off more rapidly than the experimental curves in the inner region and more slowly in the outer region. The calculated jet lengths are in good agreement with the experimental values for an unheated jet, but tend to be greater than the experimental results for the heated jet at large jet speeds relative to ambient velocity.

The dependence of jet length, axial velocity, and axial temperature upon initial jet temperature is obtained for both planar and round jets, and the results are consistent with those obtained for a submerged nonisothermal jet.

Unclassified

SECURITY CLASSIFICATION OF THIS PAGE(When Data Entered)

Preface

The author would like to thank Mr. Bruce A. Kunkel for his critical review and constructive criticism of the final manuscript.

ACCESSION for		
NTIS	White Section	<input checked="" type="checkbox"/>
DDC	Buff Section	<input type="checkbox"/>
UNANNOUNCED		<input type="checkbox"/>
JUSTIFICATION _____		
BY _____		
DISTRIBUTION/AVAILABILITY CODES		
Dist.	AvAIL.	and/or SPECIAL
A		

Contents

1. INTRODUCTION	7
2. JET GEOMETRY	8
3. VELOCITY AND TEMPERATURE PROFILES	9
4. AXIAL DISTRIBUTION OF VELOCITY AND TEMPERATURE	10
4.1 Initial Section Analysis for Mass and Momentum	10
4.2 Main Section Analysis for Mass and Momentum	13
4.3 Temperature Analysis for Main Section	15
5. METHOD OF SOLUTION	16
6. MODIFICATION OF SOLUTION	19
7. EFFECT OF JET HEATING UPON DYNAMIC CHARACTERISTICS OF JET	22
8. RESULTS AND DISCUSSION	23
9. SUMMARY AND CONCLUSIONS	26
REFERENCES	27
LIST OF SYMBOLS	29

Illustrations

1. Schematic Representation of Geometry of Counterflowing Jet and Velocity and Temperature Profiles 9
2. Comparison of Calculated Velocity Distributions Along Jet Axis With Corresponding Experimental Curves 24
3. Comparison of Calculated Temperature Distributions Along Jet Axis With Corresponding Experimental Curves 25
4. Comparison of Calculated Jet Length x_2 With Experimental Result at Several Values of m 26

Interaction of a Turbulent Planar Heated Jet with a Counterflowing Wind

1. INTRODUCTION

To aid in the development of an operational warm fog dispersal system (WFDS), experimental and theoretical studies have been made of the characteristics of ground-based heated jets for various combinations of heat and thrust under different wind conditions. The dynamic characteristics and trajectories of buoyant heated jets in a coflowing wind have been presented in previous reports.^{1, 2, 3} In references 1 and 2, the characteristics of planar and round jets were obtained; in reference 3, a method was developed for taking into account the attachment of the jet to the ground for a considerable portion of the jet trajectory (ground effect).

The dynamic characteristics of non-buoyant coflowing jets are well known and were presented in detail by Abramovich.⁴ The principle problem, therefore, in determining the trajectory of a heated coflowing jet is to properly evaluate the

(Received for publication 26 September 1977)

1. Klein, M. M., and Kunkel, B. A. (1975) Interaction of a Buoyant Turbulent Planar Jet With a Co-Flowing Wind, AFCRL-TR-75-0368.
2. Klein, M. M., and Kunkel, B. A. (1975) Interaction of a Buoyant Turbulent Round Jet With a Co-Flowing Wind, AFCRL-TR-75-0581.
3. Klein, M. M. (1977) A Method for Determining the Point of Lift-Off and Modified Trajectory of a Ground-Based Heated Turbulent Planar Jet in a Co-Flowing Wind, AFGL-TR-77-0033.
4. Abramovich, G. N. (1963) The Theory of Turbulent Jets, The MIT Press, Cambridge, Mass., Chaps. 4 and 9.

buoyant force. The situation for the counterflowing jet, as presented by Abramovich,⁴ is considerably less satisfactory for both theory and experiment because the calculations that must account for the regions of counterflow are quite specialized and not easily adaptable to the buoyant jet. Recently, however, a simplified model was presented by Sekundov⁵ for a counterflowing round jet, and it can be extended in a straightforward way to take account of buoyancy and obtain the jet trajectories. An important feature of the Sekundov model is the use of a finite wall to help simplify the equations of motion. The results for an open jet are then obtained by making the wall diameter arbitrarily large.

Because Sekundov limits himself to the unheated incompressible jet, the model must first be extended to take account of density variation. In addition, an energy equation must be developed to help determine the temperature distribution along the jet axis. The effect of buoyancy upon the jet characteristics will be presented in a subsequent report. Since the jets in a warm fog dispersal system merge a short distance downstream of the jet nozzles,⁶ the analysis has been confined to the planar case.

2. JET GEOMETRY

A schematic sketch of the flow pattern for a planar jet in a counterflowing wind is shown in Figure 1. The jet issues with a velocity u_o and starts mixing with the counterflowing stream of velocity u_a , resulting in a boundary layer that grows inward toward the center of the jet. This region, called the initial section, terminates when the boundary layer reaches the center of the jet. The surface $y_1(x)$, where x is horizontal position and y the vertical coordinate, separates the regions of unperturbed and perturbed flow in this initial section.

The velocity profile remains constant in the next interval, known as the main section. The surface $y_2(x)$ separates the region in which the flow has retained its original direction from that in which the flow has been reversed. Thus, at y_2 the velocity is zero. Analogous to the surface y_1 in the initial section, the surface $y_3(x)$ separates the regions of perturbed and unperturbed flow for the opposing stream. The line y_3 is, therefore, a streamline of the flow.

Because of the constricting effect of the walls, the unperturbed velocity u_c in the main region is slightly greater than u_a . Experiment indicates that the flow

-
5. Sekundov, A. N. (1969) The propagation of a turbulent jet in an opposing stream, in Turbulent Jets of Air, Plasma, and Real Gas, Consultants Bureau, New York, A Division of Plenum Publishing Corp., N. Y. 10011.
 6. Kunkel, B. A. (1975) Heat and Thrust Requirements of a Thermal Fog Dispersal System, AFCRL-TR-75-0472.

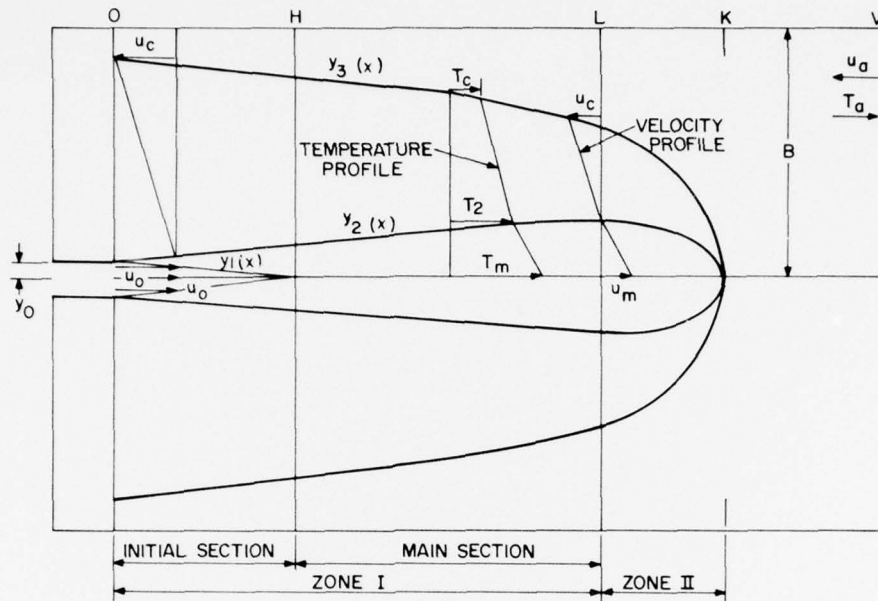


Figure 1. Schematic Representation of Geometry of Counterflowing Jet and Velocity and Temperature Profiles

regime in a counterflowing jet can be separated into two zones. In zone I, consisting of the initial and main sections, the pressure is fairly constant and the surface y_2 grows at a constant rate. In zone II, the pressure starts to rise rapidly, the surface y_2 starts to decrease, and the final retardation of the jet flow is attained. Since at this point the axial velocity u_m is comparable in magnitude to the stream velocity, we may, for convenience, here take u_m as numerically equal to u_a .

Because of the large pressure rise in zone II, the velocity and temperature distributions in this regime cannot be accurately calculated. However, since these quantities do not differ greatly from their free-stream values, simple interpolation may be used where required.

3. VELOCITY AND TEMPERATURE PROFILES

Following Sekundov we shall utilize a linear profile for the transverse velocity distribution and will assume, in addition, that the temperature profile is a linear function of the velocity profile. The use of linear profiles considerably simplifies the analysis, and should, as is usually the case with integral methods, have only a weak effect upon the final results. For the region between the axis and y_2 , we write the velocity and temperature distributions in the form

$$\frac{u}{u_m} = 1 - y/y_2 \quad (1)$$

$$\frac{T - T_c}{T_m - T_c} = \frac{u + u_c}{u_m + u_c} \quad (2)$$

where subscript m refers to values along the axis and subscript c to the unperturbed flow above y_3 .

At $y = y_2$, $u = 0$ so that the temperature T_2 at y_2 is given by

$$\frac{T_2 - T_c}{T_m - T_c} = \frac{u_c}{u_m + u_c} \quad (3)$$

For the region between y_2 and y_3 , the profiles have the form

$$\frac{u}{u_c} = \frac{y - y_2}{y_3 - y_2} \quad (4)$$

$$\frac{T - T_c}{T_2 - T_c} = \frac{u_c - u}{u_c} = 1 - \frac{y - y_2}{y_3 - y_2} \quad (5)$$

4. AXIAL DISTRIBUTION OF VELOCITY AND TEMPERATURE

4.1 Initial Section Analysis for Mass and Momentum

Conservation of mass and momentum between the beginning of the initial section, O, and section V to the right of zone II yields

$$\rho_o u_o y_o + \rho_a u_a b - \int_{y_2}^{y_3} \rho u dy - \rho_c u_c (b - y_3) = 0 \quad (6)$$

$$\rho_o u_o^2 y_o - \rho_a u_a^2 b = - \int_{y_2}^{y_3} \rho u^2 dy - \rho_c u_c^2 (b - y_3) + (p_a - p_c) b \quad (7)$$

where ρ is the density, p the pressure, and the subscript o refers to initial jet values. Since y_3 is a streamline of the flow, the pressure, density, and velocity in the region above y_3 are related by the Bernoulli equation for channel flow,

$$\int \frac{dp}{\rho} + \frac{u^2}{2} = \text{const} \quad (8)$$

In the development of the conservation equations, we will be interested in the limiting form of these equations as the wall width becomes large. In the region above y_3 , a typical quantity, that is, density ρ_c , may be replaced by ρ_a , except where the limiting form $(\rho_a - \rho_c)$ occurs. We now show that the only limiting form of consequence is that containing the velocity, the others being negligible. To evaluate the integral in Eq. (8), we utilize the adiabatic law

$$\frac{p}{\rho^\gamma} = \text{const} \quad (9)$$

where γ is the ratio of specific heats, yielding

$$\frac{\gamma}{\gamma-1} \frac{p_a}{\rho_a^\gamma} \left(\rho_a^{\gamma-1} - \rho_c^{\gamma-1} \right) = \frac{u_c^2}{2} - \frac{u_a^2}{2} \quad (10)$$

Since ρ_c is close to ρ_a , we may express ρ_c in the form

$$\rho_c = \rho_a - (\rho_a - \rho_c)$$

and expand ρ_c to first order in the small difference $\rho_a - \rho_c$ to yield

$$\frac{\rho_a - \rho_c}{\rho_a} = \frac{1}{2\gamma} \frac{\rho_a}{p_a} (u_c^2 - u_a^2) \sim \frac{1}{\gamma} \frac{\rho_a}{p_a} u_a^2 \frac{(u_c - u_a)}{u_a} \quad (11)$$

From the adiabatic law, Eq. (9), the pressure difference is given by

$$\frac{p_a - p_c}{p_a} = \gamma \frac{(\rho_a - \rho_c)}{\rho_a} \quad (12)$$

while from the perfect gas law,

$$p = \rho R T \quad (13)$$

the temperature difference is

$$\frac{T_a - T_c}{T_a} = \frac{p_a - p_c}{p_a} - \frac{(\rho_a - \rho_c)}{\rho_a} = (\gamma - 1) \frac{(\rho_a - \rho_c)}{\rho_a} \quad (14)$$

For a typical case, $u_a = 20$ m/sec (moderately high speed jet), $p_a = 1$ atm, $T_a = 287^\circ\text{K}$, $\rho_a = 0.00123$ gm/cm³, and the coefficient on the right side of Eq. (11) has the value

$$\frac{1}{\gamma} \frac{\rho_a}{p_a} u_a^2 = 0.00348 \quad .$$

Thus, the density difference and, from Eqs. (12) and (14), the pressure and temperature difference are all small compared to the velocity difference. We may therefore replace ρ_c and T_c by ρ_a and T_a and write the pressure difference in the form

$$p_a - p_c = \frac{\rho_a}{2} (u_c^2 - u_a^2) \quad (15)$$

Because of the virtual constancy of the pressure in zone I, the integrals in Eqs. (6) and (7) can, by use of the perfect gas law, be easily evaluated. However, the logarithmic forms introduced by the integrals makes the equations awkward to handle in subsequent analysis. Since we are interested in small to moderate temperature and density differences, we will, for convenience and simplification, utilize an arithmetic mean for the density difference and write

$$\text{average } \frac{\rho}{\rho_m} = a_1 = \frac{1}{2} \frac{(\rho_2 + \rho_m)}{\rho_m} \quad , \quad 0 \leq y \leq y_2 \quad (16)$$

$$\text{average } \frac{\rho}{\rho_a} = a_o = \frac{1}{2} \frac{(\rho_2 + \rho_a)}{\rho_a} \quad , \quad y_2 \leq y \leq y_3 \quad (17)$$

The mass and momentum, Eqs. (6) and (7), now take the form

$$\rho_o u_o y_o + \rho_a u_a b - \rho_a u_a \frac{(y_3 - y_2)}{2} a_o - \rho_a u_c b + \rho_a u_c y_3 = 0 \quad (18)$$

$$\rho_o u_o^2 y_o - \rho_a u_a^2 b = -\rho_a u_a^2 \frac{(y_3 - y_2)}{3} a_o - \rho_a u_c^2 b + \rho_a u_a^2 y_3 + \frac{1}{2} \rho_a (u_c^2 - u_a^2) b \quad (19)$$

At this point we take all quantities as dimensionless, referring to ambient values for density, velocity, and temperature and to the initial jet width, y_o , for length. The mass and momentum equations may now be written as

$$(u_c - 1)b = \rho_o m - \frac{(y_{30} - y_{20})}{2} a_o + y_{30} \quad (20)$$

$$\rho_o m^2 = -\frac{a_o}{3}(y_{30} - y_{20}) + y_{30} - \frac{1}{2}(u_c^2 - 1)b \quad (21)$$

where m is used for the dimensionless initial jet velocity, u_o , and y_{30} and y_{20} indicate initial values of y_3 and y_2 . Since $y_{20} = 1$, Eqs. (20) and (21) may be solved for the unknowns y_{30} and $(u_c - 1)b$ to yield

$$y_{30} = \frac{6 m \rho_a}{a_o} (m + 1) + 1 \quad (22)$$

$$\begin{aligned} (u_c - 1)b &= \rho_o m + y_{30} \left(1 - \frac{a_o}{2}\right) + \frac{a_o}{2} \\ &= \frac{3}{a_o} (2 - a_o) \rho_o m^2 + \frac{2}{a_o} (3 - a_o) \rho_o m + 1 \quad (23) \end{aligned}$$

4.2 Main Section Analysis for Mass and Momentum

The conservation equations for the region between a typical section L in the main region and section V are

$$\int_0^{y_2} \rho u \, dy + b - \int_{y_2}^{y_3} \rho u \, dy - u_c \rho_c (b - y_3) = 0 \quad (24)$$

$$\int_0^{y_2} \rho u^2 \, dy - b = - \int_{y_2}^{y_3} \rho u^2 \, dy - \rho_c u_c^2 (b - y_3) + (p_a - p_c)b \quad (25)$$

which, after use of Eq. (15) and integration of the profile distributions, may be written as

$$\rho_m u_m a_1 \frac{y_2}{2} - y_2 (N - 1) \frac{a_0}{2} - (u_c - 1)b + N y_2 = 0 \quad (26)$$

$$\rho_m u_m^2 \frac{a_1}{3} y_2 = - (N - 1) \frac{a_0}{3} y_2 - (u_c^2 - 1) \frac{b}{2} + N y_2 \quad (27)$$

where $N = y_3/y_2$. We may unite Eq. (26) in the more compact form

$$\left[\frac{\beta}{2} + N \left(1 - \frac{a_0}{2} \right) \right] y_2 = \alpha \quad (28)$$

where

$$\beta = \rho_m u_m a_1 + a_0 \quad (29)$$

$$\alpha = (u_c - 1)b \quad (30)$$

Use of Eq. (28) for α in Eq. (27) yields

$$\frac{\beta}{2} + N \left(1 - \frac{a_0}{2} \right) = N - (N - 1) \frac{a_0}{3} - \rho_m u_m^2 \frac{a_1}{3} \quad (31)$$

which may be solved for N in the form

$$N = 2 \frac{a_1}{a_0} \rho_m u_m^2 + 3 \frac{a_1}{a_0} \rho_m u_m + 1 \quad (32)$$

Since α has been obtained from its value at the initial section, Eq. (23), and is assumed constant throughout the main section, Eqs. (28) and (32) provide the distribution of axial velocity and the coordinate y_3 , if the axial temperature T_m is known. From Eqs. (23) and (28) we may write the velocity distribution in the more explicit form

$$\left[\frac{\beta}{2} + N \left(1 - \frac{a_0}{2} \right) \right] y_2 = \frac{\rho_0}{a_0} [3(2 - a_0)m^2 + 2(3 - a_0)m] + 1 \quad (33)$$

4.3 Temperature Analysis for Main Section

To obtain the temperature distribution in the main section, we calculate the transport of energy between sections L and V and obtain, analogous to the transport of mass in Eq. (24),

$$\int_0^{y_2} \rho u T dy - \int_{y_2}^{y_3} \rho u T dy - u_c \rho_c T_c (b - y_3) = -b \quad (34)$$

Expressing T in terms of temperature excess over ambient, $\Delta T = T - 1$, and making use of the mass equation, we can write Eq. (34) in the equivalent form

$$\int_{y_2}^{y_3} \rho u \Delta T dy - \int_0^{y_2} \rho u \Delta T dy = \rho_c u_c (1 - T_c) (b - y_3) \quad (35)$$

The term $1 - T_c$ can, with the aid of Eqs. (11) and (14), be represented in terms of the velocity difference $\Delta u_c = u_c - 1$ by

$$\begin{aligned} 1 - T_c &= \frac{\gamma - 1}{\gamma} \frac{1}{RT_a} \Delta u_c u_a^2 \\ &= \frac{u_a^2}{C_p T_a} \Delta u_c \end{aligned} \quad (36)$$

where C_p is the specific heat of the gas, taken as constant. Utilizing Eq. (28), expressing ρ in terms of T by the gas law, and noting that the term y_3 is negligible compared to b for a wide jet, the energy equation can be written in the form

$$\int_{y_2}^{y_3} u \left(1 - \frac{1}{T}\right) dy - u_m \int_0^{y_2} \frac{u}{u_m} \left(1 - \frac{1}{T}\right) dy = \frac{u_a^2 y_2}{C_p T_a} \left[\frac{\beta}{2} + N \left(1 - \frac{a_0}{2}\right) \right] \quad (37)$$

Parallel to the treatment of the density term in Eqs. (6) and (7), we replace $1/T$ by its corresponding arithmetic mean μ to give

$$(1 - \mu_1) \int_{y_2}^{y_3} \frac{u}{u_c} dy - u_m(1 - \mu_2) \int_0^{y_2} \frac{u}{u_m} dy = \frac{u_a^2}{C_p T_a} y_2 \left[\frac{\beta}{2} + N \left(1 - \frac{a_o}{2} \right) \right] \quad (38)$$

where

$$\mu_1 = \frac{1}{2} \left(1 + \frac{1}{T_2} \right), \quad y_2 - y_3 \text{ interval} \quad (39)$$

$$\mu_2 = \frac{1}{2} \left(\frac{1}{T_m} + \frac{1}{T_2} \right), \quad 0 - y_2 \text{ interval} .$$

Performing the integration we obtain

$$(N - 1) \frac{\Delta T_2}{T_2} - u_m \left(\frac{\Delta T_m}{T_m} + \frac{\Delta T_2}{T_2} \right) = \frac{4u_a^2}{C_p T_a} \left[\frac{\beta}{2} + N \left(1 - \frac{a_o}{2} \right) \right] \quad (40)$$

which, together with Eqs. (28) and (32), allows us to calculate temperature, velocity, and the coordinate y_3 along the main section. The coordinate y_2 occurring in these equations is a simple linear function of x given by

$$y_2 = cx \quad (41)$$

where c is a constant having the value 0.27 for the initial section and 0.22 for the main region.

5. METHOD OF SOLUTION

Although we have simplified the analysis by the use of average values for temperature and density, the solution for the foregoing equations is quite complex for the general case. However, for the case of small to moderate heating the equations can be further simplified and explicit solutions obtained. The quantity ΔT_m is initially comparable to unity but decreases very rapidly and becomes small in the earlier portion of the main region. The term ΔT_2 is always small compared to unity. Thus, the coefficient a_o , Eq. (17),

$$a_o = \frac{1}{2} \left(\frac{1}{T_2} + 1 \right) \sim 1 - \frac{\Delta T_2}{2}, \quad (42)$$

is close to unity. If we write Eq. (33) in the form

$$\left[\frac{\beta}{2} + N \left(1 - \frac{a_o}{2} \right) \right] y_2 = \frac{\rho_o}{a_o} [2(1 - a_o) + 4m + 3(1 - a_o)m^2 + 3m^2] + 1 \quad (43)$$

and use the initial value of ΔT_2 from Eq. (3),

$$\Delta T_{20} = \frac{\Delta T_o}{1+m}, \quad (44)$$

and note that, for the test data analyzed, m is large compared to unity, we can write Eq. (43) in the approximate form

$$\left[\frac{\beta}{2} + N \left(1 - \frac{a_o}{2} \right) \right] y_2 = \frac{\phi_o(m)}{T_o} \quad (45)$$

where

$$\phi_o(m) = 3m^2 + 4m + 1 + 3(1+m) \Delta T_o. \quad (46)$$

Utilizing Eq. (32) for the value of N , Eq. (31) may be written as

$$\frac{\beta}{2} + N \left(1 - \frac{a_o}{2} \right) = \frac{a_1}{a_o} \rho_m \left[u_m^2 + 2u_m + \left(1 - \frac{a_o}{2} \right) (u_m^2 + u_m) \right] + 1 \quad (47)$$

in which, from Eqs. (16) and (17), a_1/a_o is given by

$$\frac{a_1}{a_o} = \frac{1 + \frac{\Delta T_m}{2} \left(\frac{2 + u_m}{1 + u_m} \right)}{1 + \Delta T_2}. \quad (48)$$

Since $\Delta T_2 = \Delta T_m / (1 + u_m)$ is a small term, we can approximate Eq. (48) by

$$\frac{a_1}{a_o} = 1 + \frac{\Delta T_m}{2} \quad (49)$$

and reduce Eqs. (47) and (32) to the form

$$\frac{\beta}{2} + N \left(1 - \frac{a_o}{2}\right) = \frac{(u_m + 1)^2}{1 + \Delta T_m} \left[1 + \frac{\Delta T_m}{2} \left(1 + \frac{1}{1 + u_m}\right)\right] \quad (50)$$

$$N = \frac{(u_m + 1)/(2u_m + 1)}{1 + \Delta T_m} \left[1 + \frac{\Delta T_m}{2} \left(\frac{2 + u_m}{1 + u_m}\right)\right] \quad (51)$$

The velocity equation (45) and the energy equation (40) may now be written as

$$(u_m + 1)^2 y_2 = \frac{1 + \Delta T_m}{1 + \frac{\Delta T_m}{2} \left(1 + \frac{1}{1 + u_m}\right)} \frac{\phi_o(m)}{T_o} \quad (52)$$

$$\Delta T_m = \frac{4u_a^2}{C_p T_a} \frac{\left(1 + \frac{3}{2} \Delta T_m\right) (u_m + 1)^2}{(1 + \Delta T_m) u_m} \left[1 + \frac{\Delta T_m}{2} \left(1 + \frac{1}{1 + u_m}\right)\right] \quad (53)$$

The velocity equation (52) and the energy equation (53) may be solved simultaneously in the form of cubic equations for the velocity and temperature as functions of jet position. A much simpler solution may be obtained, however, by noting that ΔT_m drops off rapidly in the initial region of the jet and, therefore, the temperature terms on the right-hand side of Eqs. (52) and (53) have only a small effect upon the velocity and temperature distributions. We therefore neglect these terms in obtaining initial solutions and write Eqs. (52) and (53) in the form

$$(u_m + 1)^2 y_2 = \frac{\phi_o(m)}{T_o} \quad (54)$$

$$\Delta T_m u_m = \frac{4u_a^2}{C_p T_a} (u_m + 1)^2 \quad (55)$$

which give simple solutions for u_m and ΔT_m as functions of x . It is convenient to refer Eqs. (54) and (55) to the end of the initial section x_H at which $u_m = m$, $\Delta T_m = \Delta T_o$, and write

$$(u_m + 1)^2 = (m + 1)^2 \frac{x_H}{x} \quad (56)$$

$$\frac{\Delta T_m}{\Delta T_o} = \frac{(u_m + 1)^2}{u_m} \frac{m}{(m + 1)^2} \quad (57)$$

where x_H is, by Eq. (54), obtained from

$$x_H = \frac{1}{0.27} \frac{\phi_o(m)}{(m + 1)^2 T_o} \quad (58)$$

Similarly, the end of the main section x_1 , at which $u_m = 1$, is given by

$$x_1 = \frac{1}{0.22} \frac{\phi_o(m)}{4T_o} \quad (59)$$

The initial solution for the temperature obtained from Eq. (57) may now be utilized in Eqs. (52) and (53) to obtain more accurate solutions for the velocity and temperature. Calculations indicated that the temperature correction has a small effect upon the temperature distribution and a negligible effect upon the velocity. It may be noted that Eq. (57) for the temperature distribution is close to that for the coflowing jet,

$$\Delta T_m \sim u_m + 1 \quad ,$$

at small to moderate jet distances, but yields somewhat larger values in the outer region of the jet where u_m becomes comparable to unity.

6. MODIFICATION OF SOLUTION

Utilizing the analysis of Abramovich (Ref. 4, Chap. 9, pp 391-416), the length of zone II is given in terms of the length x_1 of zone I by, approximately,

$$x_2 - x_1 = 0.176 x_1 \quad (60)$$

An analysis of the test data obtained at Irvine, California, during 1974 (Kunkel⁶) shows that the calculated jet length, x_2 , obtained from Eq. (60) is too large, by about a factor of 2, compared to the corresponding experimental values, particularly at the large values of m . This is in contradistinction to the results for the opposing round jet in which Sekundov⁵ obtains jet lengths that are in good agreement with the experimental values. Part of the discrepancy may stem from the fact that we have a two-dimensional flow that is more sensitive to small changes in velocity than an axisymmetric flow. We therefore modify the analysis that was used previously to determine the value of u_c from the boundary conditions at the beginning of the initial section and account for the situation at the end of the main section.

The continuity equation for the region above y_3 , between the initial section O and an arbitrary section in the main region,

$$\rho_c u_c = \rho_{co} u_{co} \frac{(b - y_{30})}{b - y_3} \quad (61)$$

yields for large b

$$(u_c - 1)b = (u_{co} - 1)b + y_3 - y_{30} \quad (62)$$

in which the density variation is dropped since it is small compared to the velocity change. Use of Eqs. (23) and (28) yields

$$\left[\frac{\beta}{2} + N \left(1 - \frac{a_o}{2} \right) \right] y_2 = \frac{2m}{T_o} + 2y_3 - y_{30} \quad (63)$$

The coordinate y_3 may be calculated from Eq. (51) for N and Eq. (52) for y_2 to give

$$y_3 = \frac{(m+1)(3m+1)}{1+u_m} \frac{1 + \frac{3\Delta T_o}{3m+1}}{1 + \Delta T_o} \frac{2u_m + 1}{1 + \Delta T_m} \left[1 + \frac{\Delta T_m}{2} \left(\frac{2 + u_m}{1 + u_m} \right) \right] \quad (64)$$

in which we note the term $3\Delta T_o/(3m+1)$ is small compared to unity. Evaluating Eq. (64) at $u_m = 1$ and noting that here ΔT_m is small, we get

$$y_3 = \frac{3}{2} \frac{(m+1)(3m+1)}{1 + \Delta T_o} \quad (65)$$

Utilizing Eq. (65) for y_3 and Eq. (22) for y_{30} , Eq. (63) takes the form

$$(u_m + 1)^2 y_2 = \frac{1 + \Delta T_m}{1 + \frac{\Delta T_m}{2}} \frac{\phi_1(m)}{\left(1 + \frac{1}{1 + u_m}\right) T_o} \quad (66)$$

where

$$\phi_1(m) = \frac{3m^2 + 8m + 3}{2} \quad (67)$$

Since the right-hand side of Eq. (66) is approximately 1/2 that of Eq. (52), the corrected value of x_1 is about 1/2 the value. This correction brings the calculated jet length into closer agreement with the corresponding experimental value. However, the velocity u_m is now too small, especially in the earlier region of the jet. This situation is not surprising, since we now have a solution that is accurate at x_1 but does not satisfy the condition $u_m = m$ at x_H . We therefore utilize a linear combination of the unmodified and the modified solutions that reduces to Eq. (52) at x_H and to Eq. (66) at x_1 ; that is,

$$(1 + u_m)^2 y_2 = \left[\frac{\phi_o(m)}{T_o} \frac{x_1 - x}{x_1 - x_H} + \frac{\phi_1(m)}{T_o} \frac{x - x_H}{x_1 - x_H} \right] \frac{1 + \Delta T_m}{1 + \frac{\Delta T_m}{2}} \quad (68)$$

in which we neglect the small term $1/(1 + u_m)$ in the temperature correction. It is convenient to express Eq. (68) in terms of the parameters x_H and x_1 and write

$$(1 + u_m)^2 = \left[\frac{(1 + m)^2}{\left(\frac{1 + \Delta T_o}{1 + \Delta T_o/2}\right)} \frac{x_H}{x} \frac{x_1 - x}{x_1 - x_H} + \left(\frac{4}{1 + \Delta T_1}\right) \frac{x_1}{x} \frac{x - x_H}{x_1 - x_H} \right] \times \frac{1 + \Delta T_m}{1 + \Delta T_m/2} \quad (69)$$

where x_H and x_1 are related to $\phi_o(m)$ and $\phi_1(m)$ by

$$x_H = \frac{\phi_o(m)}{(1 + m)^2} \frac{1}{c} \frac{1}{1 + \Delta T_o/2} \quad (70)$$

$$x_1 = \frac{\phi_1(m)}{4cT_0} \frac{1 + \Delta T_1}{1 + \Delta T_1/2} \quad (71)$$

and ΔT_1 is the value of ΔT_m at $u_m = 1$.

As an alternative to the use of Eqs. (70) and (71) for x_H and x_1 in Eq. (68), we may regard x_H and x_1 as experimentally determined parameters for calculating the velocity. Since the temperature distribution is given directly in terms of velocity, Eq. (53) may be used unaltered in calculating the modified temperature distribution.

7. EFFECT OF JET HEATING UPON DYNAMIC CHARACTERISTICS OF JET

The foregoing analysis shows clearly the effect of heating upon the jet characteristics. From Eq. (68) we see that the velocity decreases as $T_0^{-1/2}$ while Eq. (55) indicates that ΔT decreases roughly as $T_0^{-1/2}$. The length of zone I, x_1 , and, hence, the jet length x_2 decrease, according to Eq. (70), as T_0^{-1} . The effect of heating upon velocity and jet length for a round jet can easily be deduced from Sekundov's work by noting that the initial heating term introduces the density term $\rho_0 \sim 1/T_0$ into the term $\phi_0(m)$. Sekundov's velocity equation (2-29) may therefore be written as

$$x^2 \psi(u_m) \sim \frac{1}{T_0} \phi_0(m) \quad ,$$

where $\psi(u_m)$ is a quadratic in u_m . Thus, the velocity and jet length both decrease roughly as $T_0^{-1/2}$. Similarly, it is easy to show from conservation of energy for a round jet, analogous to Eqs. (33) and (37), that the temperature drops off as $T_0^{-1/2}$.

As indicated by Sekundov,⁵ the dependence of jet length upon temperature for a round opposing jet may easily be deduced by noting that the propagation characteristics of zone I are similar to those of a submerged jet, and zone I is the major region of an opposing jet. In this way, using conservation of momentum and energy for a submerged nonisothermal jet, we obtain,

for a round jet:

$$x^2 u_m^2 \sim \rho_0$$

$$\Delta T_m u_m x^2 \sim \rho_0 \quad ,$$

for a plane jet:

$$x u_m^2 \sim \rho_0$$

$$\Delta T_m u_m x \sim \rho_0 ,$$

from which the previously obtained dependence of jet length, velocity, and temperature upon initial jet temperature for both plane and round jets is immediately deduced.

8. RESULTS AND DISCUSSION

The calculated velocity and temperature distributions for several Irvine tests are shown in Figures 2 and 3 along with the corresponding experimental curves. These results cover most of the range of initial jet speed, initial jet temperature, and ambient wind encountered in the tests. In general, the calculated results are in fair to good agreement with the experimental results. The calculated velocity drops off too rapidly in the initial region of the jet, but tends to approach the experimental value at larger jet distances. The calculated temperatures also drop off somewhat too rapidly in the initial region of the jet, but then they decrease slowly enough to give temperatures higher than the experimental values. These results are consistent with those obtained for the coflowing jet (Klein³).

The slower decrease of the experimental values of temperature and velocity in the early portion of the jet are probably due to incomplete mixing, resulting in higher maximum values of velocity and temperature at a given location. A possible factor contributing to the more rapid outer-region decrease in the experimental curves of velocity and temperature is the buoyant motion of the jet that results in more rapid mixing than occurs for a horizontal nonbuoyant jet.

Several values of the jet length x_2 obtained by the present method are shown in Figure 4 as a function of m , along with the corresponding experimental results. In addition, the experimental values obtained by Timma⁷ for an incompressible unheated jet are presented to indicate the trend at low values of m . In order not to complicate the results due to heating, the experimental and calculated results have been restricted to initial excess temperatures less than 30 percent of ambient temperatures. The calculated values appear to follow the trend indicated by the results of Timma, while the experimental results are somewhat lower. The

7. Timma, E. (1962) Turbulent circular and planar jets in an opposing stream, Izv. Est. SSR, Ser. Techn. i. Fiz.-Mat. Nauk, 11 (No. 4).

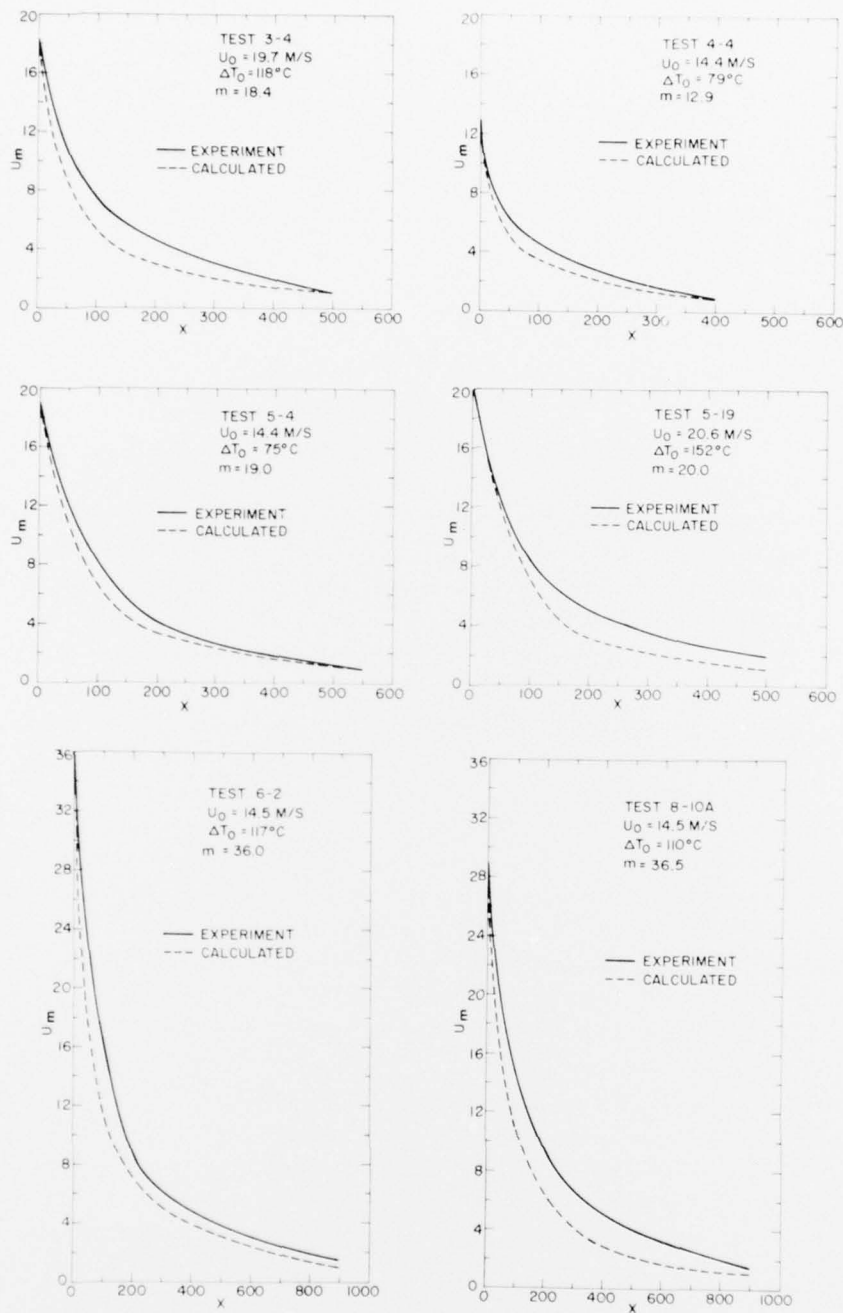


Figure 2. Comparison of Calculated Velocity Distributions Along Jet Axis With Corresponding Experimental Curves

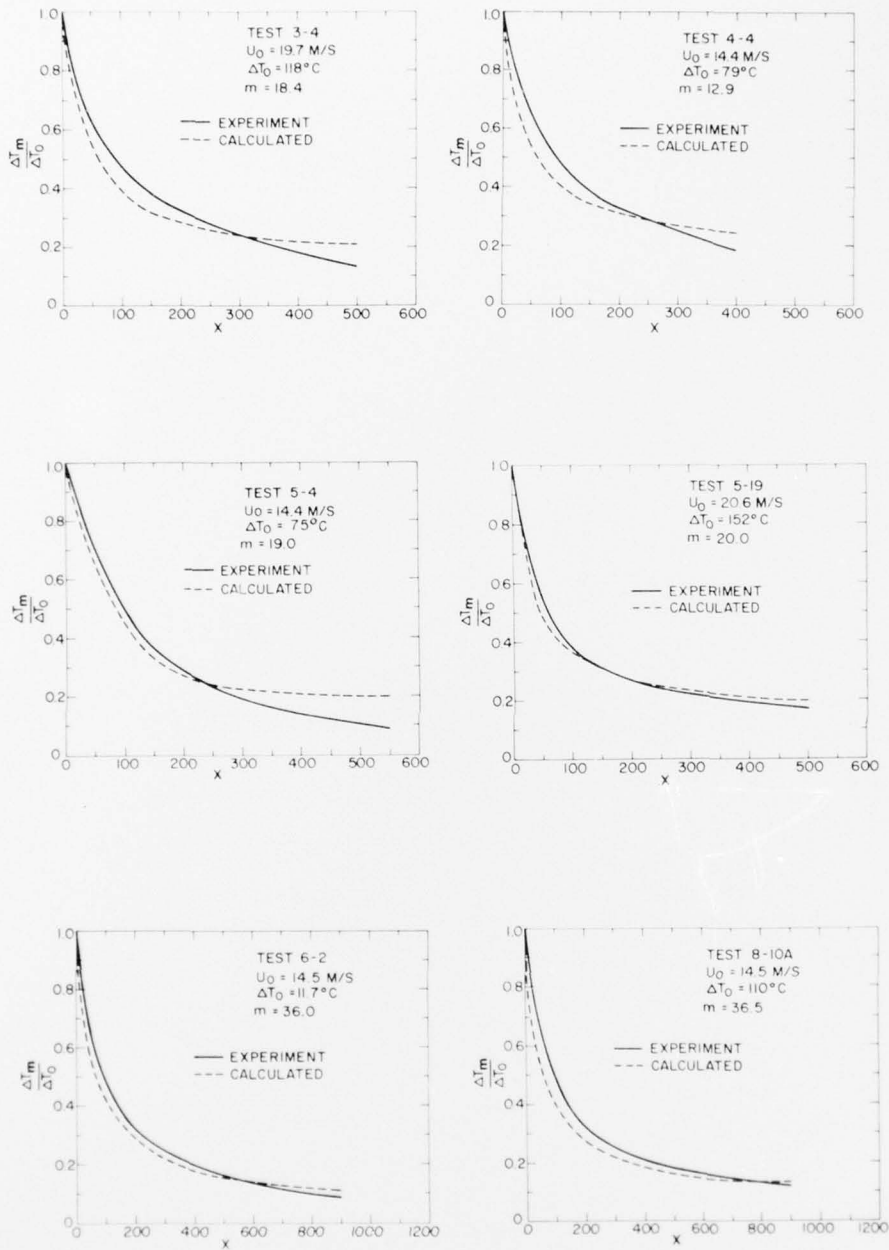


Figure 3. Comparison of Calculated Temperature Distributions Along Jet Axis With Corresponding Experimental Curves

lower experimental values are probably due, in part, to the buoyancy, which tends to decrease the jet length.

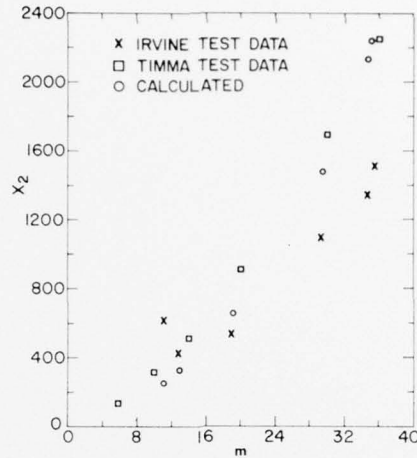


Figure 4. Comparison of Calculated Jet Length x_2 With Experimental Result at Several Values of m

9. SUMMARY AND CONCLUSIONS

The method developed by Sekundov⁵ to calculate the dynamic characteristic of an incompressible round jet in an opposing stream has been extended to the case of a heated planar jet. The calculated velocity and temperature distributions along the jet axis are in fair to good agreement with the experimental results. In general, the calculated velocity and temperature values drop off too rapidly in the early portion of the jet, while the temperature decreases too slowly in the outer region. The calculated jet lengths are consistent with experimental values for unheated low velocity jets, but tend to be higher than the experimental results for heated high velocity jets.

The analysis shows that for a planar jet the velocity and temperature decrease as $T_o^{-1/2}$, while the jet length drops off as T_o^{-1} . For a round heated jet the velocity, jet length, and temperature all decrease as $T_o^{-1/2}$. These results are consistent with those obtained by simple dimensional analysis of the conservation laws for momentum and energy for a submerged nonisothermal jet.

References

1. Klein, M. M., and Kunkel, B. A. (1975) Interaction of a Buoyant Turbulent Planar Jet With a Co-Flowing Wind, AFCRL-TR-75-0368.
2. Klein, M. M., and Kunkel, B. A. (1975) Interaction of a Buoyant Turbulent Round Jet With a Co-Flowing Wind, AFCRL-TR-75-0581.
3. Klein, M. M. (1977) A Method for Determining the Point of Lift-Off and Modified Trajectory of a Ground-Based Heated Turbulent Planar Jet in a Co-Flowing Wind, AFGL-TR-77-0033.
4. Abramovich, G. N. (1963) The Theory of Turbulent Jets, The MIT Press, Cambridge, Mass., Chaps. 4 and 9.
5. Sekundov, A. N. (1969) The propagation of a turbulent jet in an opposing stream, in Turbulent Jets of Air, Plasma, and Real Gas, Consultants Bureau, New York, A Division of Plenum Publishing Corp., N. Y. 10011.
6. Kunkel, B. A. (1975) Heat and Thrust Requirements of a Thermal Fog Dispersal System, AFCRL-TR-75-0472.
7. Timma, E. (1962) Turbulent circular and planar jets in an opposing stream, Izv. Est. SSR, Ser. Techn. i. Fiz.-Mat. Nauk, 11 (No. 4).

List of Symbols

b	distance from outside wall to jet axis
c	jet thickness coefficient
H	end of initial section
m	wind speed parameter (u_o/u_a)
L	arbitrary position in main section
O	initial position in main section
p	pressure
T	jet temperature
T_a	ambient temperature
T_m	temperature on axis
ΔT	temperature excess over ambient ($T - T_a$)
u	jet velocity
V	arbitrary section in main stream
x	horizontal position along jet
y	vertical position
y_o	jet half-width
y_1	zero velocity surface in initial section

y_2 zero velocity surface in main section
 y_3 surface separating perturbed and unperturbed flows
 ρ gas density

Subscripts

a ambient
c region above y_3 surface
m on jet axis
o initial jet position